

# Phonon confinement effects in diffusive quantum transport simulations with the effective mass approximation and k·p method

Anne Ziegler and Mathieu Luisier

Integrated Systems Laboratory, ETH Zürich, CH-8092 Zurich, Switzerland (e-mail: aziegler@ethz.ch)

**Abstract**—Despite the continuous shrinking of the transistor dimensions, advanced modeling tools going beyond the ballistic limit of transport are still critically needed to ensure accurate device investigations. For that purpose we present here a straightforward approach to include phonon confinement effects into dissipative quantum transport calculations based on the effective mass approximation (EMA) and the k·p method. The idea is to scale the magnitude of the deformation potentials describing the electron-phonon coupling to obtain the same low-field mobility as with full-band simulations and confined phonons. This technique is validated by demonstrating that after adjusting the mobility value of *n*- and *p*-type silicon nanowire transistors, the resulting EMA and k·p *I*-*V* characteristics agree well with those derived from full-band studies.

## I. INTRODUCTION

Ultra-scaled nanowire transistors have been identified as a promising evolution of the current FinFET technology and might play an important role in the future of the semiconductor industry [1]. To support their design accurate computer-based modeling tools are required. Due to the low dimensions of the nanowire channel and the resulting strong confinement and quantization effects, a quantum mechanical description of the simulation domain should be a key ingredient of the selected approach. This can be achieved, for example, via the Non-equilibrium Green's Function (NEGF) formalism. Furthermore, it has been shown that even with gate lengths below 15 nm, silicon-based ultra-scaled devices still do not operate at the ballistic limit of transport. This is not only due to fabrication-related issues, e.g. surface roughness or alloy disorder, but also to intrinsic phenomena such as electron-phonon interactions. It is therefore essential to include these dissipative mechanisms in order to satisfactorily capture the physics of next-generation transistors [2].

The choice of the Hamiltonian matrix that represents the structure of interest is also a critical parameter. On one hand, atomistic tight-binding (TB) models reproduce the bandstructure of most semiconductors very well and allow to account for confined phonons, but the incurred computational burden is large [3]. On the other hand, the continuous effective mass approximation (EMA) and k·p methods help drastically decrease the simulation time, but sometimes at the expense of the physical accuracy, e.g. electrons usually interact with bulk phonons [4], which can no more be justified at the nanometer scale. Hence, in this paper a straightforward technique is proposed to mimic the influence of confined phonons in EMA- and k·p-based quantum transport solvers. The idea consists in scaling the deformation potential energy describing the electron-phonon coupling in order to obtain the same low-field mobility as with confined phonons and TB calculations. After

this initial parameterization step, the *I*-*V* characteristics of *n*- and *p*-type silicon nanowire transistors with transport along the <100>, <110>, and <111>-oriented can be accurately simulated, the results from EMA (electrons) and k·p (holes) being in good agreement with the tight-binding ones.

The paper is organized as follows: in Section II the modeling of electron-phonon scattering and the proposed method to adjust the strength of this interaction are discussed. In Section III we apply the proposed method to a circular silicon nanowire field-effect transistor (NW FET). Transport calculations are performed for channel lengths of 5 nm for both *n*- and *p*-type devices and compared to accurate, but computationally more intensive full-band results [5]. Finally, Section IV summarizes the paper and its main contributions.

## II. METHOD

The transport properties of nanoscale devices can be directly calculated from the Schrödinger equation (SE) by introducing open boundary conditions [6]

$$(E - H - \Sigma^{RB}(E)) \cdot \Psi(E) = \text{Inj}(E), \quad (1)$$

where  $H$  is the device Hamiltonian,  $\Sigma^{RB}(E)$  the boundary self-energy that connect the simulation domain with its environment, and  $\text{Inj}(E)$  an injection vector. The unknowns are the wave functions  $\Psi(E)$ . Here, the electron and hole bandstructures of the considered Si nanowires are described by an effective mass  $H^{EMA}$  and 6-band k·p  $H^{6 \times 6}$  Hamiltonian [4] Hamiltonian, respectively, both discretized on a finite difference grid. Eq. (1) is solved for all possible electron/hole energies, the results integrated to give the carrier density, which is self-consistently coupled to the Poisson equation. While this formalism is computationally very efficient, it is restricted to ballistic simulations. To account for electron-phonon scattering, as intended here, the NEGF formalism has to be recalled, whose governing equations are

$$(E - H - \Sigma^{RB}(E) - \Sigma^{RS}(E)) \cdot G^R(E) = I, \quad (2)$$

$$G^{\gtrless} = G^R(E) \cdot (\Sigma^{\gtrless B}(E) + \Sigma^{\gtrless S}(E)) \cdot G^A(E). \quad (3)$$

The first one refers to the retarded Green's function, the second one to the greater and lesser one. The electron-phonon interactions are cast into scattering self-energies  $\Sigma^S(E)$ , which are assumed to be diagonal and whose lesser and greater components at discretization point  $i$  are given by [3]

$$\Sigma_{ii}^{\gtrless S}(E) = \sum_l M_l^2 \left( N_{ph}(\omega_l) G_{ii}^{\gtrless}(E \pm \hbar\omega_l) + (N_{ph}(\omega_l) + 1) G_{ii}^{\gtrless}(E \mp \hbar\omega_l) \right). \quad (4)$$

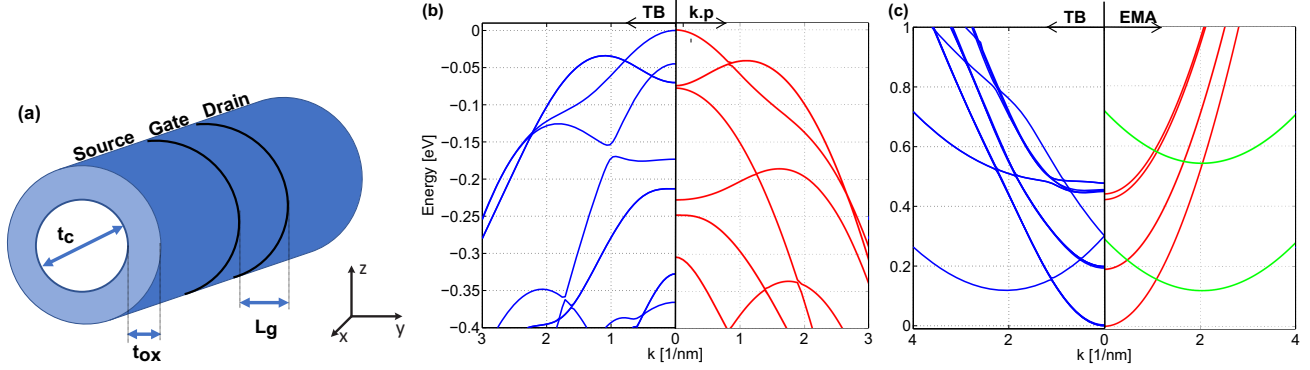


Fig. 1. (a) Schematic view of the  $n$ - and  $p$ -type, silicon gate-all-around nanowire field-effect transistors considered in this work. The total length is set to 35 nm with a gate length  $L_g=5$  nm and a body diameter of  $d=3$  nm. The source and drain extensions are doped with a donor (acceptor) concentration  $N_{D(A)}=1e20$  cm $^{-3}$ . The high- $\kappa$  oxide surrounding the channel has a thickness of  $t_{ox}=3$  nm. (b) Valence band of the  $\langle 100 \rangle$ -oriented Si nanowire as computed with tight-binding (left) and 6-band k-p with adjusted Luttinger parameters (right). (c) Same as (b), but for the conduction band and the EMA on the right axis. The band extrema have been moved to  $E=0$  eV.

Note that the  $\Sigma_{ii}^{RS}(E)$  are derived from the lesser and greater components above as in Ref. [3]. Here,  $N_{ph}(\omega_l)$  is the Bose-Einstein distribution of the phonon with frequency  $\omega_l$ ,  $G^{\gtrless}(E)$  the greater (lesser) Green's function at energy  $E$ , and  $M_l$  the coupling strength between carriers and the bulk phonon mode  $l$ . When  $\omega=0$ ,  $\Sigma_{ii}^{\gtrless S}(E)$  reduces to  $M_{ac}^2 G_{ii}^{\gtrless}(E)$ . The acoustic and optical coupling strengths are defined as

$$M_{ac} = D_{ac} \cdot \sqrt{\frac{k_B T}{\rho v_s^2}} \quad (5)$$

$$M_{op} = D_{op} \cdot \sqrt{\frac{3\hbar}{\rho \omega_{opt}}}, \quad (6)$$

respectively, where  $D_{ac(op)}$  is the acoustic (optical) deformation potential (DF),  $k_B$  the Boltzmann constant,  $\hbar$  Plank's reduced constant,  $T$  the temperature of the system,  $\omega_{op}$  the optical phonon energy,  $v_s$  the sound velocity, and  $\rho$  the mass density of the material.

To take the influence of phonon confinement effects into account in the continuous EMA and k-p approaches, the bulk acoustic and optical deformation potential energies [7] are multiplied by a factor  $F$  whose value is adjusted till phonon-limited mobility results computed within the nearest-neighbor  $sp^3d^5s^*$  tight-binding model are precisely reproduced [8]. In this scheme, the confined DF's can be related to the bulk ones via the following equation

$$D_{ac(op),conf.} = F \cdot D_{ac(op),bulk}. \quad (7)$$

All the low-field electron and hole phonon-limited mobilities,  $\mu_{ph}$ , are determined with the  $dR/dL$  method [9], which implies that the transistor channel resistance  $R$  linearly increases with the sample length  $L$

$$\mu_{ph} = \left[ \frac{dR(L)}{dL} \right]^{-1} \cdot \frac{1}{q P_{inv}(N_{inv})}, \quad (8)$$

with  $dR(L)/dL$  being the derivative of the total device resistance with respect to its length. In case of diffusive transport and long enough sample length, this quantity is independent of  $L$ . Finally,  $P_{inv}$  and  $N_{inv}$  represent the hole and electron concentration in the middle of the nanowire channel, respectively, while  $q$  is the elementary charge.

### III. RESULTS

The proposed method has been applied to the simulation of  $\langle 100 \rangle$ -,  $\langle 110 \rangle$ -, and  $\langle 111 \rangle$ -oriented  $n$ - and  $p$ -type gate-all-around silicon NW FETs. The source and drain extensions of the chosen structure measure  $L_s=L_d=15$  nm with a donor or acceptor doping concentration of  $1e20$  cm $^{-3}$ , the gate length is equal to  $L_g=5$  nm, and the nanowire diameter is set to  $d=3$  nm, as depicted in Figure 1(a). The high- $\kappa$  oxide layer surrounding the channel has a thickness  $t_c=3$  nm and a relative dielectric constant  $\epsilon_R=20$ . Here, gate leakage currents are neglected. They are anyhow expected to be very small. Electrons and holes are injected into the device at the source and drain contacts only and propagate along the  $x$ -axis, which is defined as the transport direction. In this configuration  $y$  and  $z$  are directions of confinement.

As a first step, by directly extracting the electron effective masses from full-band calculations and deriving the Luttinger parameters from the original values given in Ref. [10], the conduction and valence bandstructures of the Si NW have been adjusted to best match the tight-binding ones, as indicated exemplarily for the device with transport along the  $\langle 100 \rangle$  axis in Figure 1(b-c). The same qualitative agreement has been obtained for the other crystal orientations. The electron and hole bulk deformation potentials have been taken from [7], [11], [12] (see Table I).

As mentioned above, to compute the low-field electron and hole phonon-limited mobility  $\mu_{ph}$  with the  $dR/dL$  method, the transistor channel resistance must linearly increase with the sample length. This is confirmed in Figure 2(a) for the  $n$ -type NW FETs and in subplot (b) for the  $p$ -type ones. For that purpose, the  $n$ -type device length had to be set to  $20 \leq L_{device,n} \leq 40$  nm, while it could be made shorter for the  $p$ -type devices ( $12 \leq L_{device,n} \leq 20$  nm) due to a higher carrier-phonon coupling strength and therefore a shorter mean free path for scattering  $\lambda$ . If  $L < \lambda$ , the resistance increase might not be linear because the magnitude of the electron-phonon interactions might be too weak. Figure 3 reports the computed electron (a) and hole (b) low-field phonon-limited mobilities  $\mu_{ph}$  for different values of the scaling factor  $F$  (from 0.25 to 1.5) that scales all the bulk deformation potentials (acoustic and optical) for electrons

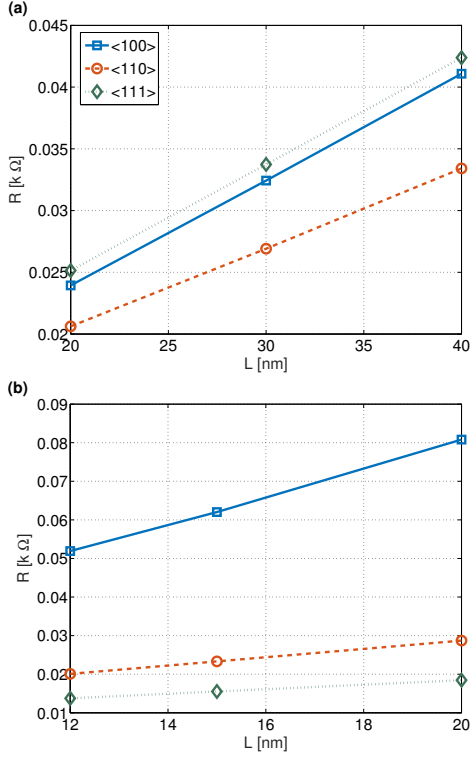


Fig. 2. Channel resistance of the (a)  $n$ - and (b)  $p$ -type Si NW FETs with transport along the  $\langle 100 \rangle$ ,  $\langle 110 \rangle$  and  $\langle 111 \rangle$  crystal axis, as computed with the EMA and k-p method, respectively. A constant flat potential and bulk deformation potentials are assumed in these calculations.

(holes) equally as indicated in Eq. (7). The EMA (k-p method) have been used to determine the electron (hole) values. A non-linear dependence of  $\mu_{ph}$  on  $F$  can be observed due to the presence of the square of  $M_l$  in the scattering self-energy in Eq. (4). The EMA and k-p mobilities have then been compared to full-band results and the DF factor  $F$  that gives the best agreement extracted. Both is summarized in Table II. It clearly appears that  $F$  must be made orientation- and type-dependent in order to match the tight-binding reference data.

TABLE I. ACOUSTIC  $\Xi_{ac}$  AND OPTICAL  $DK_{op}$  BULK DEFORMATION POTENTIALS FOR ELECTRONS  $e$  AND HOLES  $h$  USED IN THIS PAPER. THE VALUES HAVE BEEN TAKEN FROM [7], [11], [12]).

Type	DF	Value	Units
n-type Si	$\Xi_{ac}^e$	9.0	eV
	$DK_{op,g3}^e$	11.0	eV/Å
	$\hbar\omega_{g3}$	63.0	meV
	$DK_{op,f3}^e$	2.0	eV/Å
	$\hbar\omega_{f3}$	63.0	meV
p-type Si	$\Xi_{ac}^h$	10.2	eV
	$DK_{op}^h$	15.0	eV/Å
	$\hbar\omega$	63.0	meV

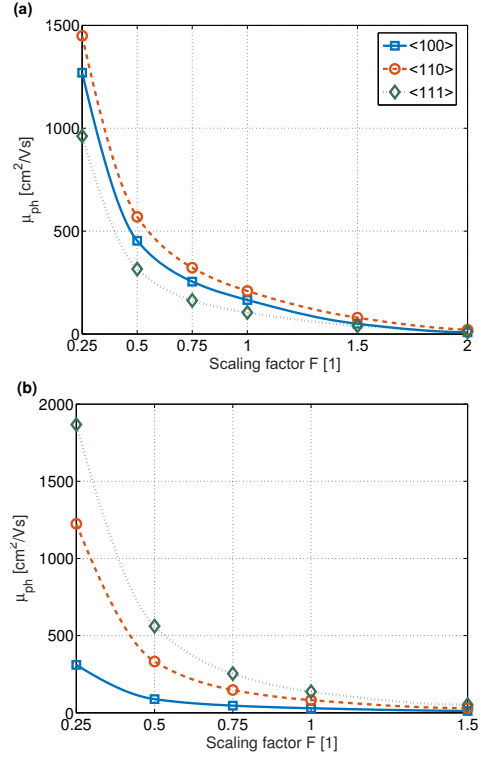


Fig. 3. Electron (a) and hole (b) low-field phonon-limited mobility for the considered crystal orientations as a function of the factor  $F$  scaling the acoustic and optical deformation potential energies. The non-linear dependence of  $\mu_{ph}$  on  $F$  is due to the squared deformation potential in the scattering self-energy.

As next step, the validity of the simulation approach can be tested by simulating the  $I_d$ - $V_{gs}$  transfer characteristics of Si NW FETs with the EMA and k-p method, either in the ballistic limit of transport or in the presence of electron-phonon scattering with the scaling factor  $F$  established from the mobility calculations. It is expected that the “current vs. voltage” agree very well with the full-band tight-binding data for both transport types (ballistic and diffusive) because the bandstructures and scattering parameters have been first carefully adjusted. This is demonstrated in Figure 4, where the transfer characteristics of the  $n$ - and  $p$ -type  $\langle 100 \rangle$  devices are shown. A similar behavior is obtained for the other crystal orientations that have been analyzed in this work, as summarized in Table II. The ON current magnitudes calculated with adjusted deformation potentials agree much better with the TB results than those evaluated with bulk phonon parameters, except for the  $p$ -type  $\langle 111 \rangle$ -oriented Si nanowire for which  $I_{ON,conf\ ph}$  significantly exceeds  $I_{ON,TB}$ . The cause of this discrepancy can be traced back to the nanowire bandstructure: due to the short gate length considered here ( $L_g=5$  nm), a substantial part of the OFF-state leakage current comes from source-to-drain tunneling. Since the 6-band k-p model does not contain any information about the conduction band of the simulated material, it tends to overestimate the value of the decaying factor responsible for the tunneling processes. As a consequence, the S-to-D tunneling leakage is underestimated in our k-p calculations, the inverse sub-threshold slope becomes steeper, and the ON-current larger. A perturbative treatment as in Ref. [13] is currently investigated to get rid of this issue.

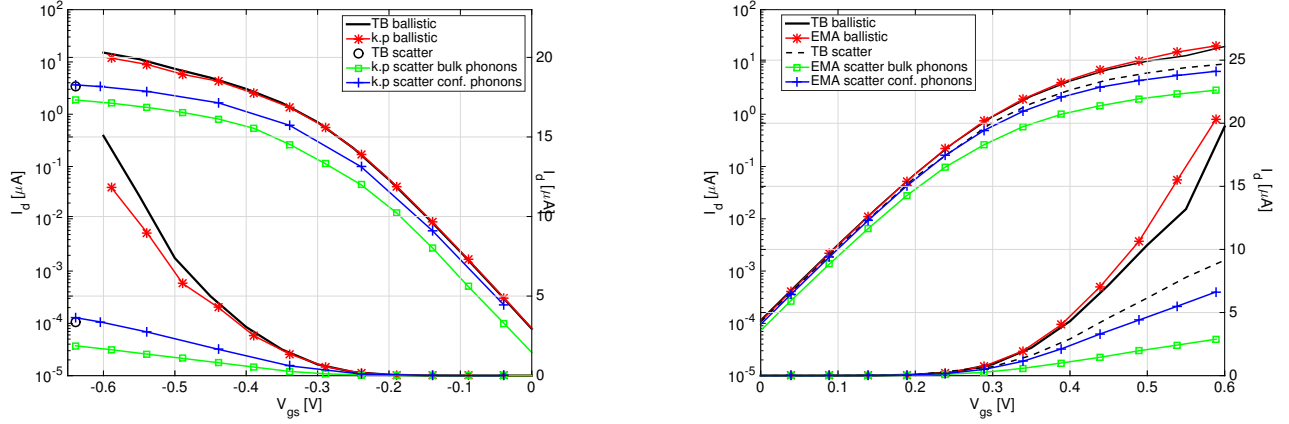


Fig. 4. Transfer characteristics  $I_d$ - $V_{gs}$  at  $V_{ds}=0.6$  V of the (a)  $p$ - and (b)  $n$ -type  $\langle 100 \rangle$  nanowire transistor in Fig. 1. The devices have been simulated with a full-band tight-binding simulator (black lines) as reference. The  $p$ -type ( $n$ -type) characteristics have been computed with a  $k$ - $p$  (EMA) solver in the ballistic regime (red stars) and in the presence of electron-phonon interactions (green squares: bulk phonons, blue crosses: confined phonons).

#### IV. CONCLUSION

We have presented a computationally efficient method to deal with quantum transport in  $n$ - and  $p$ -type Si nanowire transistors within the EMA and  $k$ - $p$  method, in the presence of electron-phonon scattering and under the influence of confined phonons. In order to achieve good reproduction of tight-binding results the bulk deformation potential has been scaled according to low-field mobility values computed with tight-binding. The method has been applied to silicon nanowire transistors. It has been found that the required scaling factor  $F$  depends on both the crystal orientation and carrier type, probably also on the nanowire diameter. Hence, parameterizations of  $F$  with full-band mobility calculations seem unavoidable each time a new structure shall be simulated.

TABLE II. PHONON-LIMITED MOBILITY  $\mu_{ph}$  TAKEN FROM FULL-BAND RESULTS, DEFORMATION POTENTIAL SCALING FACTOR  $F$  AND ON CURRENT VALUES IN  $[\mu\text{A}]$  WITH BULK ( $I_{ON,BULK PH}$ ) AND CONFINED ( $I_{ON,CONF PH}$ ) PHONONS FOR  $n$ - AND  $p$ -TYPE SI NW FETs COMPARED TO TIGHT-BINDING RESULTS ( $I_{ON,TB}$ ).

	n-type Si			p-type Si		
	$\langle 100 \rangle$	$\langle 110 \rangle$	$\langle 111 \rangle$	$\langle 100 \rangle$	$\langle 110 \rangle$	$\langle 111 \rangle$
$\mu_{ph}$ [cm <sup>2</sup> /Vs]	304.0	541.8	123.7	47.1	802.9	1907
$F$	0.68	0.53	0.9	0.75	0.35	0.25
$I_{ON,TB}$	9.01	8.7	6.1	4.2	10.3	10.4
$I_{ON,bulk ph}$	2.8	4.5	2.3	1.8	5.1	7.7
$I_{ON,conf ph}$	6.6	9.0	6.7	3.6	12.0	18.2

#### ACKNOWLEDGMENT

This work was supported by SNF Grant No. PP00P2\_159314 and by a grant from the Swiss National Supercomputing Centre under Project No. s662.

#### REFERENCES

- [1] N. P. Dasgupta, J. Sun, C. Liu, S. Brittan, S. C. Andrews, J. Lim, H. Gao, R. Yan, and P. Yang, "25th anniversary article: semiconductor nanowires—synthesis, characterization, and applications," *Advanced Materials*, vol. 26, no. 14, pp. 2137–2184, 2014.
- [2] M. Rau, E. Caruso, D. Lizzit, P. Palestri, D. Esseni, A. Schenk, L. Selmi, and M. Luisier, "Performance projection of iii-v ultra-thin-body, finfet, and nanowire mosfets for two next-generation technology nodes," in *Electron Devices Meeting (IEDM), 2016 IEEE International*. IEEE, 2016, pp. 30–6.
- [3] M. Luisier and G. Klimeck, "Atomistic full-band simulations of silicon nanowire transistors: Effects of electron-phonon scattering," *Physical Review B*, vol. 80, no. 15, p. 155430, 2009.
- [4] N. Cavassilas, F. Michelini, and M. Bescond, "Multiband quantum transport simulations of ultimate p-type double-gate transistors: Effects of hole-phonon scattering," *Journal of Applied Physics*, vol. 109, no. 7, p. 073706, 2011.
- [5] M. Luisier, A. Schenk, W. Fichtner, and G. Klimeck, "Atomistic simulation of nanowires in the s p 3 d 5 s\* tight-binding formalism: From boundary conditions to strain calculations," *Physical Review B*, vol. 74, no. 20, p. 205323, 2006.
- [6] M. Luisier and A. Schenk, "Two-dimensional tunneling effects on the leakage current of mosfets with single dielectric and high-gate stacks," *Electron Devices, IEEE Transactions on*, vol. 55, no. 6, pp. 1494–1501, 2008.
- [7] J. Li, E. Lampin, C. Delerue, and Y.-M. Niquet, "Theoretical investigation of the phonon-limited carrier mobility in (001) si films," *Journal of Applied Physics*, vol. 120, no. 17, p. 174301, 2016.
- [8] M. Luisier, "Phonon-limited and effective low-field mobility in n-and p-type [100]-, [110]-, and [111]-oriented si nanowire transistors," *Applied Physics Letters*, vol. 98, no. 3, p. 032111, 2011.
- [9] K. Rim, S. Narasimha, M. Longstreet, A. Mocuta, and J. Cai, "Low field mobility characteristics of sub-100 nm unstrained and strained si mosfets," in *Electron Devices Meeting, 2002. IEDM'02. International*. IEEE, 2002, pp. 43–46.
- [10] M. Shin, S. Lee, and G. Klimeck, "Computational study on the performance of si nanowire pmosfets based on the  $k$ - $p$  method," *IEEE Transactions on Electron Devices*, vol. 57, no. 9, pp. 2274–2283, 2010.
- [11] C. Jacoboni and L. Reggiani, "The monte carlo method for the solution of charge transport in semiconductors with applications to covalent materials," *Reviews of Modern Physics*, vol. 55, no. 3, p. 645, 1983.
- [12] D. Rode, "Low-field electron transport," *Semiconductors and semimetals*, vol. 10, pp. 1–89, 1975.
- [13] A. Ziegler, M. Frey, L. Smith, and M. Luisier, "A nonparabolic bandstructure model for computationally efficient quantum transport simulations," *IEEE Transactions on Electron Devices*, vol. 63, no. 5, pp. 2050–2056, 2016.